Charge Density and Bonding in Bis(diiminosuccinonitrilo)nickel, $Ni(C_4N_4H_2)_2$: A Combined Experimental and Theoretical Study

Chi-Shen Lee, Tsong-Song Hwang, Yu Wang,* Shie-Ming Peng, and Ching-Shan Hwang

Department of Chemistry, National Taiwan University, Taipei, Taiwan, R.O.C.

Received: July 12, 1995; In Final Form: October 15, 1995[⊗]

A combined experimental and theoretical charge density study is made on the compound bis(diiminosuccinonitrilo)nickel, Ni(s-disn)$_2$. It is investigated experimentally by an accurate X-ray diffraction measurement on a single crystal of the compound at 110 K and theoretically by various molecular orbital calculations. The crystal belongs to monoclinic crystal system, space group $P2_1/n$; $a = 3.639(1)$, $b = 8.743(1)$, $c = 15.948(1)$ Å, $\beta = 94.74(1)°$, $Z = 2$. The molecule is planar with pseudo-D_{2h} symmetry stacked along the a axis. Single-point MO calculations are performed using EHMO, ab initio, and density functional methods. Deformation densities are produced via conventional $X-X_{high}$, multipole model, and MO calculations. Bonding densities along N−H, C−C, C−N, C≡N bonds, and lone-pair electron densities are clearly demonstrated and are in excellent agreement between experiment and theory. The bonding density between the coordinated nitrogen atom of the ligand and the nickel atom indicates a certain degree of dative bond through the donation of nitrogen lone pair electrons to the metal center. The redistribution in electron density around the nickel atom is substantial with electron density depletion along the σ-direction but electron density surplus along the π-direction, which conforms to the crystal field theory. The agreement in deformation density between experiment and theory around nickel atom is reasonably good. Bonding type in the s-disn ligand was further analyzed with orbital wave functions, the complete π-electron delocalization of the ligand is incorporated with the d_{xz}, d_{yz} orbitals of the Ni atom. Three Lewis structures are deduced from the ab initio MO calculation; they are exactly the same as expected by valence bond theory. The resonance between three Lewis structures represents the π-electron delocalization of the molecule. Comparisons between experiment and theory are made on electron density distribution, net atomic charges of the molecule, and d-orbital occupancies of the Ni atom.

Introduction

Ni(II) transition metal complexes are known to form dominantly four-coordinated planar structures. However, there are six-coordinated O_h structures, e.g., the perovskite $KNiF_3$[1] where the Ni atom is bonded to six F atoms at an exact O_h geometry (d_{Ni-F} 2.0057(4) Å). A similar structure, K_2NiF_4,[2] consists of a Ni atom at D_{4h}, again bonded to six F atoms at the same distance (2.0065(3) Å × 4; 2.0062(8) Å × 2) showing a pseudo-O_h geometry but leading to a significant difference on the electron density distribution between xy and (xz, yz) planes.[2] Another six-coordinated nickel fluoride structure, NiF_2,[3] is a rutile structure where Ni is at D_{2h} site with two types of Ni−F distances (1.997(1) Å × 2; 2.011(1) Å × 4). A tetragonal distortion with shortened axial geometry. Such distortion would certainly affect the electron density distribution around the Ni atom.[3] A square-planar structure can be considered as the extreme case of such distortion. The metalloporphyrins do play an important role in biological systems, the characteristic planar molecules are often packed in a one-dimensional stack[4] in the crystalline state. A combined experimental and theoretical study on the electronic structure of Ni(TMP) was made[5] in order to establish the quantum mechanical basis of its biological significance. Similar charge density study on the planar $Ni(S_2C_2O_2)_2^{2-}$ molecule was later reported by Maslen et al.[6]

In this paper we describe a combined experimental and theoretical study of the charge density distribution in the Ni(s-disn)$_2$ molecule. It is a planar molecule, originally synthesized by Miles et al.,[7] packed in a similar fashion as in metalloporphyrins[5] and in $Ni(S_2C_2O_2)_2^{2-}$.[6] However, it is a much simpler molecule than the metalloporphyrin, thus the Ni(s-disn)$_2$ molecule is a very interesting molecule both electronically and structually. It is an ideal case to investigate its density distribution using single-crystal X-ray diffraction and MO calculations. In addition to its similarity to metalloporphyrins, the neutral molecule is normally understood as having a Ni atom with a formal charge of 2^+ and two s-disn ligands with a formal charge of 1^- for each s-disn ligand. The monoanion, s-disn, can be obtained either by one electron reduction from the diiminosuccinonitrile or by one electron oxidation from diaminosuccinonitrile.[9a] The exact type of the coordinated ligand is in itself an interesting subject. Bond distances of this molecule[8] indicate that the ligand might be a semi-type(s-disn), i.e., a totally π-electron delocalization anionic form.[9b,c] With this charge density study, the exact bonding type of the ligand should be confirmed. The asphericity in electron density around the Ni atom due to the crystal field splitting is also of interest in the bonding of this complex. There have been a series of electron density distribution studies on the metalloporphyrins/phthalocyanins[5,11−18] where the asphericity in electron density around metal ions and/or d-orbital occupancies of the metal ion were illustrated and, in some cases, the ground state was even identified.[18] The bond order and the bond type of each bond in the molecule can be obtained through natural bonding orbital analysis in the MO calculation.

Experimental Section

Data Collection. Synthesis of Ni(s-disn)$_2$ was according to the method of Miles et al.[7] A rectangular, dark green crystal of the complex was chosen and sealed in a glass capillary for

* To whom correspondence should be addressed.
[⊗] Abstract published in *Advance ACS Abstracts,* January 15, 1996.

0022-3654/96/20100-2934$12.00/0

TABLE 1: Crystal Data. Conditions for Crystallographic Data Collection and Structure Refinement[a]

formula	$Ni\ N_8C_8H_4$
FW	135.44
diffractometer used	CAD4
space group	Monoclinic $P2_1/n$
a (Å)	3.639(1)
b (Å)	8.743(1)
c (Å)	15.948(1)
β (deg)	94.74(1)
V (Å^3)	505.7(2)
Z	2
D_{calc}(g cm^{-3})	1.779
λ (Å)	0.71069
F(000)	272
unit-cell detn: no (2θ range)	25 (40.00−60.00°)
scan type	$\theta/2\theta$
scan width (deg)	2(0.70+0.35tan(θ))
scan speed (deg/min)	1.50−8.24
2θ(max)	100.0
hkl ranges	(−7; 7)(0; 18)(0; 34)
μ (cm^{-1})	38.3
crystal size (mm)	0.20 × 0.20 × 0.22
transmission	0.62−0.74
temp (K)	110
no. of meas reflns	19814
no. of unique reflns	5224
no. of obs relfns ($I > 2.0\sigma(I)$)	3251
R_{int}	0.025
$R(F)$; $R_w(F)$	0.030; 0.031
GOF	1.91
minimized function	$\Sigma(w\|F_o - F_c\|^2)$
weights	$1/[\sigma^2(F) + 0.5 \times 10^{-4}F^2]$
g (2nd ext coeff) × 10^4	0.06(1)
$(\delta/\sigma)_{max}$	0.01
(D map)$_{max,min}$ (e/Å^3)	0.760; −0.730

[a] $R_{int} = \Sigma(I - \langle I \rangle)/\Sigma\langle I \rangle$. $R(F) = \Sigma(F_o - F_c)/\Sigma(F_o)$. $R_w(F) = \sqrt{[\Sigma(w(F_o - F_c)^2)/\Sigma(wF_o^2)]}$. $GOF = \sqrt{[\Sigma(w(F_o - F_c)^2)/(\text{no. of reflns} - \text{no. of params})]}$.

data measurement. Intensity data were collected on an Enraf-Nonius CAD4 diffractometer using Mo Kα radiation at 110 K. Experimental details are listed in Table 1, half-sphere ($\pm h,\pm k,l$) of intensity data up to 2θ of 100° were measured. In addition, four equivalent reflections with azimuthal ψ angles of −30°, −15°, 15°, 30° for each unique reflection ($\pm h,k,l$) up to 2θ of 60° were collected. There were two parts in the data: one part was collected on the original crystal (0.2 × 0.2 × 0.45 mm), and the other part was collected on somewhat smaller piece of the same crystal (0.2 × 0.2 × 0.22 mm) since the crystal was split into two pieces during the early data collection. The scale and absorption correction were treated accordingly. A total of 19 814 reflections was measured; among them, 5633 reflections were collected on the larger crystal. Each reflection was corrected for Lorentz and polarization effects. The absorption correction was made analytically with measured six faces {00±1}, {0±10}, {±10±1}. It yielded 5244 unique reflections after averaging all the equivalent reflections; the interset agreement is 0.025 (0.028 before the absorption correction). Three standard reflections were monitored every hour throughout the data measurement; the variation intensity was within ±4%.

Refinement. Conventional refinements were performed with the full-matrix least-squares processes both on full data and on high-order data (sin $\theta/\lambda > 0.70$), the function $\Sigma w|F_o - F_c|^2$ was minimized; the sigma of F_o was taken from the geometric mean of the sigmas of all equivalents. Atomic scattering factors were taken from the analytical expression in *International Table for X-ray Crystallography*, Vol. IV. An additional multipole refinement was also performed, where all the multipolar terms were expressed as a series expansion of the spherical harmonic functions.[10] A κ, value was also included for each atom type to provide the expansion/contraction of the radial distribution. Up to hexadecapoles were included for the Ni atom; up to octapole were included for non-H atoms and up to dipoles were included for H atoms. Atomic scattering factors were taken as the sum of core and valence electron contributions. All the data processing used NRCVAX programs;[36] the multipole refinements were made using the MOLLY program.[10]

Deformation Density Map. Three types of experimental deformation density maps are presented in this work: The first one is the experimental $\Delta\rho_{x-x}$, where Fourier coefficients are obtained from the difference between F_{obs} and F_{cal}, F_{cal} is calculated from the high-order (sin $\theta/\lambda \geq 0.70$) refinement, but H atoms are moved along N−H vector to make an N−H distance of 1.0 Å. The second one is a model deformation density map $\Delta\rho_{m-a}$, which is derived from a multipole model,[10] where Fourier coefficients are the difference between two F_{cal} values−one F_{cal} is calculated from a multipole model with a series expansion of spherical harmonics,[10] the other F_{cal} is only the spherical part of the model density. The third one is a static model deformation density $\Delta\rho_{m-a\ static}$, which is obtained by plotting the density in direct space according to the equation given by Hansen and Coppens,[10] where all the nuclear vibrations are excluded. To check the correctness of the model deformation density, a residual density map is normally generated after the multipole refinement. This residual density map is the difference density between the observed and the multipole model.

Parallel deformation density maps derived from various MO calculations are made by subtracting the independent spherical atomic density from the molecular density.

Molecular Orbital Calculations. The molecular geometry is taken from the X-ray diffraction result and is constrained in D_{2h} symmetry. EHMO, ab initio MO, and density functional (DFT) calculations are applied to this molecule. The corresponding deformation density distribution is derived from the difference between the total molecular density and the promolecular electron density. The total molecular density is calculated from HFSCF molecular wave functions, each occupied molecular orbital is assigned to have two electrons. The promolecular electron density is the sum of the superposition of the spherical atomic density with atoms at the same nuclear positions as they are in the molecular geometry. The spherical atomic density is calculated at ROHF/GVB level, each outer valence orbital is assigned to have equal population of electrons, e.g., $^2/_3$ and 1 for each 2p-orbital (p_x,p_y,p_z) of a carbon and a nitrogen atom, respectively. In EHMO, the basis function of Ni is taken from literature.[19] In the ab initio calculation, the basis set of Ni atom is [14,9,5]/[6,3,2] contractions.[20] The basis sets of C, H, N atoms are taken from split-valence 6-31G**. The basis set used in DFT is double numerical plus polarization (DNP),[21,24a] which is comparable to 6-31G**. The local density approximation (LDA) is applied in DFT calculation, where VWN potential[22] is used. The natural bond orbital (NBO) analysis[31] comprises a sequence of transformations from the given basis sets to various localized sets, namely, natural atomic orbitals (NAOs), natural hybrid orbitals (NHOs),[27] natural bond orbitals (NBOs), and natural localized molecular orbitals (NLMOs).[32] The NLMOs can then be transformed to the occupied MOs of HF functions:

gives basis set → NAOs → NHOs → NBOs → NLMOs

These procedures derive their names and inspiration from the natural orbitals (NOs) of Löwdin,[33] which are obtained from the diagonalization of the one-particle density matrix. The given basis functions are taken from ab initio HF calculation. The

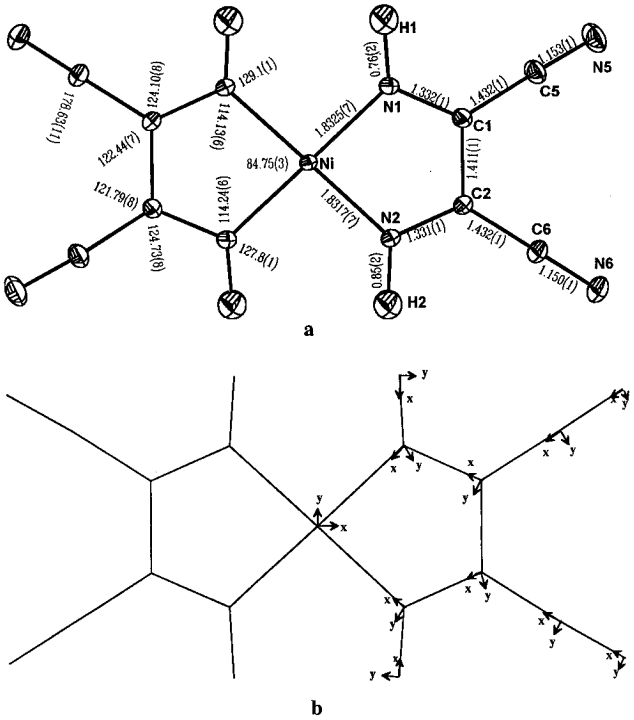

Figure 1. (a) Molecular structure of Ni(s-disn)$_2$ at 110 K, with atomic labeling, bond distances, and bond angles. (b) Definition of internal coordinates for each atom.

results after NBO analysis are generally in good agreement with Lewis structure concept and the Pauling−Slater−Coulson concept of bond hybridization and polarization. Net atomic charges, orbital occupancies, and bond orders are thus generated by means of NBO analysis; such quantities are designated as NPA[29] in comparison with the ones from Mulliken population analysis (MPA). All the ab inito and DFT computations are performed on IBM/RS6000 with GAUSSIAN92[23] and DMOL[24] programs. The EHMO calculation is made on a microvax with ICON[25] program.

Result and Discussion

Structure. The crystal structure at 110 K is the same as that at room temperature.[8] The molecule is essentially planar, and its molecular symmetry is close to D_{2h}. Its exact symmetry in solid is C_i. The molecular structure, bond distances, and bond angles are given in Figure 1a. Molecules are packed in a column along ⟨100⟩. The plane normal of the molecules makes an angle of 29.9° with the crystal *a* axis. The interplanar distance is 3.16 Å. The atomic coordinates obtained from various least-squares refinements are listed in Table 2. The Ni atom is 4-coordinated; however, as indicated previously[6] for Ni-$(S_2C_2O_2)_2^{2-}$, the planar molecules could be considered as a distorted O_h with very long axial Ni−N distance of 3.478(1) Å. Ni(II) complexes are commonly found to be planar because of its d^8 configuration. The internal coordinates of each atom in the molecule, which are used in the multipole refinement, are defined as in Figure 1b.

Refinements. In addition to the conventional refinement, multipole refinements[10] were applied to the title compound with two molecular symmetries: namely, C_i and D_{2h}. The results of these two are essentially the same. Considering the substantial reduction on the number of parameters in D_{2h} symmetry, we use the parameters thus obtained from the octapole$^+$ refinement (Table 3) for the derivation of deformation density. Additional hexadecapole terms for C and N atoms do not improve the refinement result. The agreement indexes at various stages are listed in Table 3. Significant improvement in the agreement indexes over the additional multipole terms are apparent; this indicates that the multipole model does give a better representation on the electron density distribution than the spherical model does.

TABLE 2: Atomic Parameters from Various Least-Squares Refinements[a]

atom		full data	sin(θ)/λ > 0.7	multipole
Ni	*x*	0	0	0
	y	0	0	0
	z	0	0	0
	B_{eq}	0.758(4)	0.734(8)	0.737(7)
N1	*x*	0.1691(2)	0.1692(4)	0.1687(2)
	y	0.19719(8)	0.1974(1)	0.19735(7)
	z	−0.00306(4)	−0.00324(7)	−0.00334(4)
	B_{eq}	0.96(2)	0.98(2)	1.02(2)
N2	*x*	−0.0801(2)	−0.0814(4)	−0.0812(2)
	y	0.04389(9)	0.0437(1)	0.04353(7)
	z	0.10931(4)	0.10929(6)	0.10908(4)
	B_{eq}	0.96(2)	1.00(3)	1.02(2)
N5	*x*	0.3776(3)	0.3794(9)	0.3779(3)
	y	0.5518(1)	0.5518(2)	0.55206(9)
	z	0.09194(5)	0.0919(1)	0.09193(5)
	B_{eq}	1.53(3)	1.50(5)	1.57(3)
N6	*x*	−0.1190(3)	−0.1179(7)	−0.1183(3)
	y	0.3113(1)	0.3113(2)	0.31136(9)
	z	0.27425(5)	0.2744(1)	0.27448(5)
	B_{eq}	1.71(3)	1.71(4)	1.77(3)
C1	*x*	0.1515(3)	0.1516(4)	0.1510(2)
	y	0.27360(9)	0.2737(1)	0.27356(7)
	z	0.06878(5)	0.06863(7)	0.06862(4)
	B_{eq}	0.92(2)	0.93(3)	0.98(2)
C2	*x*	0.0051(3)	0.0048(5)	0.0052(2)
	y	0.18657(9)	0.1864(1)	0.18627(7)
	z	0.13262(5)	0.13268(7)	0.13264(4)
	B_{eq}	0.93(2)	0.95(3)	1.00(2)
C5	*x*	0.2728(3)	0.2728(7)	0.2725(2)
	y	0.4282(1)	0.4277(2)	0.42771(8)
	z	0.08164(5)	0.0815(1)	0.08161(4)
	B_{eq}	1.09(3)	1.12(4)	1.17(2)
C6	*x*	−0.0598(3)	−0.0598(6)	−0.0590(2)
	y	0.2518(1)	0.2517(2)	0.25169(8)
	z	0.21246(5)	0.21241(8)	0.21224(4)
	B_{eq}	1.17(2)	1.19(3)	1.25(2)
H1	*x*	0.255(5)	0.29046	0.29046
	y	0.239(2)	0.25679	0.25679
	z	−0.039(1)	−0.05357	−0.05357
	B_{eq}	3.2(4)	2	2
H2	*x*	−0.142(5)	−0.15877	−0.15877
	y	−0.018(2)	−0.03423	−0.03423
	z	0.147(1)	0.15722	0.15722
	B_{eq}	2.1(3)	2	2

[a] $B_{eq} = (8\pi^2/3)\sum_i\sum_j u_{ij} a_i^* a_j^* a_i a_j$.

TABLE 3: Agreement indexes of Various Least-Squares Refinement (Total Number of Reflections = 5224)

	conventional	monopole	octapole+[a]	hexadecapole[b]
N_{var}[c]	80	89	157	193
$R(F)$	0.0331	0.0323	0.0238	0.0234
$R_w(F)$	0.0259	0.0212	0.0127	0.0121
$R(F^2)$[d]	0.0424	0.0393	0.0267	0.0260
$R_w(F^2)$[e]	0.0376	0.0301	0.0175	0.0162
GOF	3.153	2.584	1.572	1.507

[a] Octapole+: Ni, $l = 4$; C, N, $l = 3$; H, $l = 1$. [b] Hexadecapole: Ni, C, N, $l = 4$; H, $l = 1$. [c] N_{var}: number of variables. [d] $R(F^2) = \sum(F_o^2 - F_c^2)/\sum(F_o^2)$. [e] $R_w(F^2) = \sqrt{[\sum(w(F_o^2 - F_c^2)^2)/\sum(wF_o^4)]}$.

Deformation Density. Deformation density of the molecular plane is depicted in Figure 2. The experimental $\Delta\rho_{x-x}$ map (Figure 2a) shows clearly all the bonding densities between bonded atoms; however, it does appear noisier than the model deformation density $\Delta\rho_{m-a}$ (Figure 2b), where all the C−C, C−N, and N−H bonds are nicely presented. The density

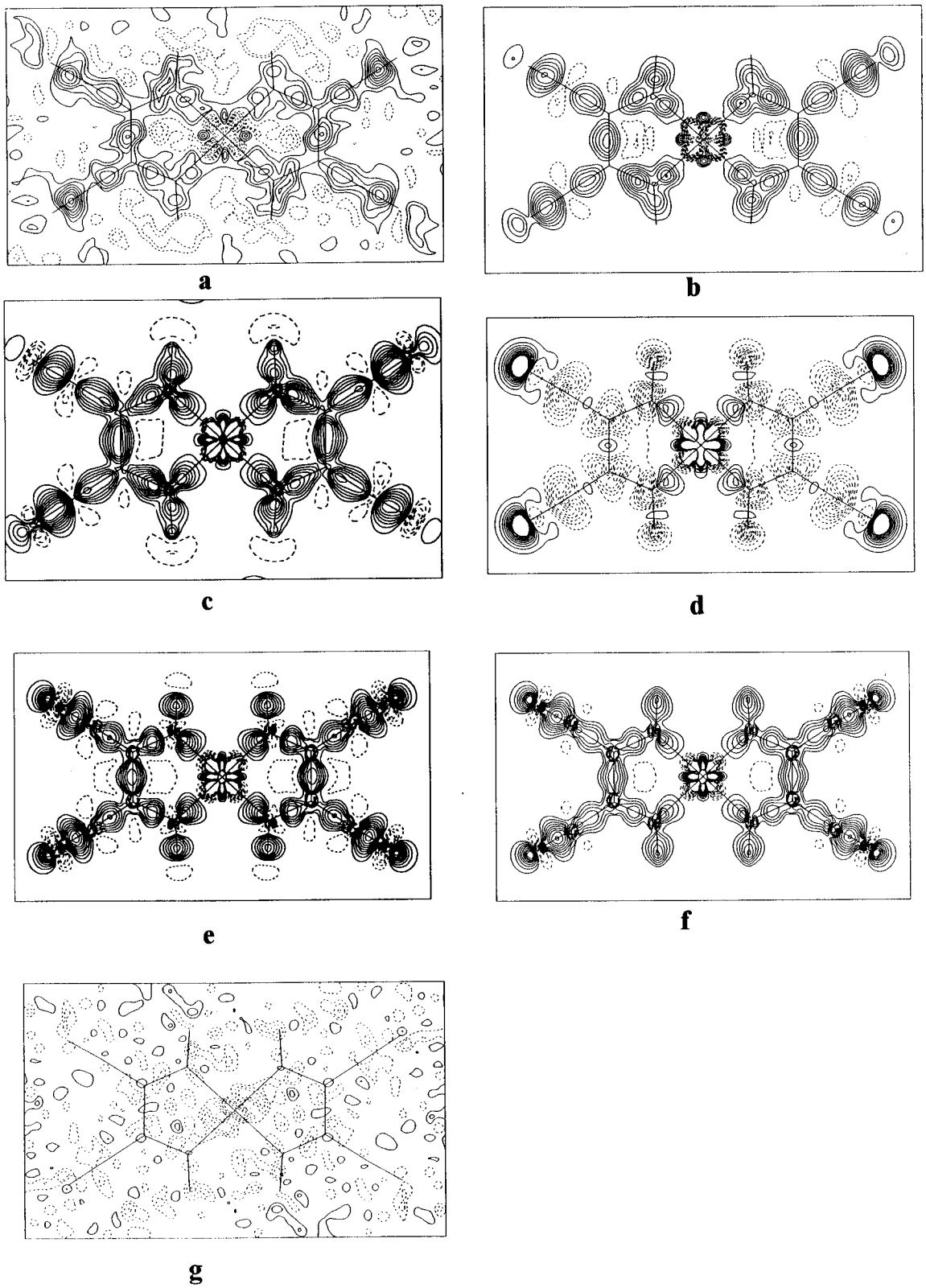

Figure 2. Deformation density maps of the molecular plane. Contours: solid line positive; dashed line zero and negative; contour interval: 0.1 e $Å^{-3}$ within ±1 e $Å^{-3}$. (a) $\Delta\rho_{x-x}$; (b) $\Delta\rho_{m-a}$; (c) $\Delta\rho_{m-a,static}$; (d)$\Delta\rho_{EHMO}$; (e) $\Delta\rho_{ab\ inito}$; (f) $\Delta\rho_{DFT}$; (g) $\Delta\rho_{residual}$.

accumulation along the C≡N triple bond is noticeably larger than the other C−N bonds in the molecule. Lone-pair electron densities of imino nitrogen atoms are pointed toward the Ni atom, which clearly demonstrate the Ni−N bond character being somewhat a dative bond. The static model deformation density map (Figure 2c) is very similar to that of model deformation density map (Figure 2b) yet with much more enhanced bonding and lone pair electron densities. Such phenomena are observed elsewhere.[2,17] Since the static map is believed to be the closest model which is assumed in molecular orbital calculations, we will present the rest of the maps in this type only. Figure 2d gives the deformation density calculated from the extended Hückel method. The appearance around the metal atom is in good agreement with both experimental and model deformation density distribution. But it does not give good comparison along C−C, C−N bonds. The results from the ab initio and the DFT

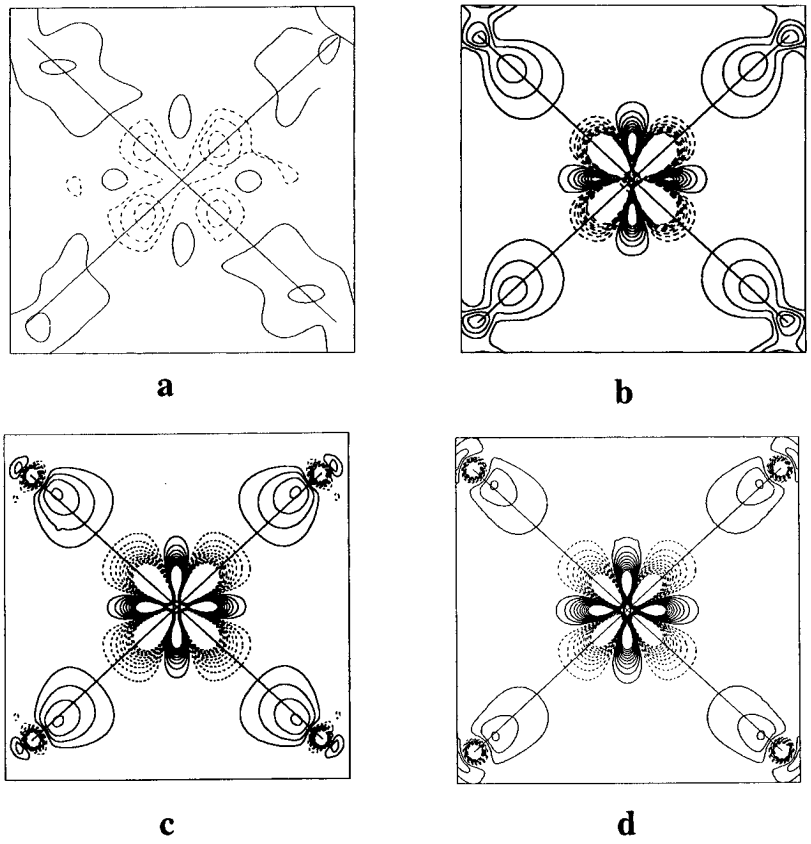

Figure 3. Same deformation density maps as in Figure 2 with enlarged NiN_4 central part. Contours interval 0.2 e Å^{-3}, within ±2 e Å^{-3}; others as in Figure 2. (a) $\Delta\rho_{x-x}$; (b) $\Delta\rho_{m-a,static}$; (c)$\Delta\rho_{ab\ inito}$; (d) $\Delta\rho_{DFT}$.

calculations shown in Figure 2e,f do give satisfactory comparison with regard to the static model deformation density (Figure 2c). The rest of deformation density maps are only showing $\Delta\rho_{x-x}$, $\Delta\rho_{m-a,\ static}$, $\Delta\rho_{ab\ initio}$, and $\Delta\rho_{DFT}$. The correctness of the multipole model is not only reflected in the improvement of the agreement indexes (Table 3) but also demonstrated in the residual density map shown in Figure 2g, where no significant feature is found. This means that the multipole model does provide the major features of the deformation density.

Deformation density distribution around the Ni atom is illustrated in three unique planes shown in Figures 3−5. The asphericity in electron density around the Ni atom is well resolved even in the experimental $\Delta\rho_{x-x}$ map, where depletion of densities are observed along the σ-directions (along Ni−N bonds) and surplus of densities are found along the π-directions (at the bisection of ∠N−Ni−N). This is exactly in accord with the prediction of the crystal field theory in a D_{2h} symmetry where electrons are populated on d_{xz}, d_{yz}, $d_{x^2-y^2}$, and d_{z^2} (note the internal coordinates defined in Figure 1b) but leave the d_{xy} orbital (σ-direction) empty. Reasonable agreement between (b), (c), and (d) in three maps (Figures 3−5) is obvious, though differences are found in Figure 5 in the region very close to the Ni nucleus, this is often true when one compares such results from experiment to theory.[15,34] Besides, the error at the nucleus (within 0.5 Å) is always higher than other region of the map.[35] The agreement between Figure 4 is very good, which clearly depicts the depletion of electron density along the σ-direction (horizontal) and surplus of electron density at the π-direction (vertical) both in static model density (Figure 4b) and in molecular orbital calculations based on ab initio and DFT (Figure 4c,d). The agreement between two calculations are also reasonably good, but not so in the other perpendicular plane (Figure 5c,d), where the horizontal axis is at the bisection of the s-disn bite angle.

If we could extend the usage of the model deformation density, the density on the plane perpendicular to the molecular plane at the midpoint of each bond of the ligand (Figure 6) can be used to analyze the π-character of the bond: the apparent cylindrical shape of density is displayed along the triple C5−N5 bond (Figure 6d) and the single C1−C5 bond (Figure 6c); a somewhat elongated shape is found along N1−C1 and C1−C2 bonds (Figure 6a,b). This provides only weak evidence of the π-electron delocalization on the s-disn ligand. The strong evidence comes from the analyses of the bonding molecular orbitals: among the bonding molecular orbitals, there are two π-molecular orbitals delocalized over the whole molecule, which are the combination of ligand p_π (p_z) orbitals and the Ni d_{xz}, d_{yz} orbitals. Wave functions of these two orbitals are depicted in Figure 7a,b; the contours are taken at 0.5 Å above the molecular plane. On the basis of these two MOs, the s-disn ligand is confirmed to be a semi-type monoanion[9b,c] with a complete π-electron delocalization on the ligand. However this monoanion ligand can be stabilized only by the metal d-orbitals (d_{xz}, d_{yz}) through the metal−ligand π-interaction.

Orbital Hybrids and Bond Orders. A natural bonding orbital analysis (NBO)[27] is applied to the ab initio MO result. Covalent bond orders can be obtained, and the corresponding Lewis structures can be drawn. Three such structures are derived based on the ab initio MO calculation. They are displayed in Figure 8 with respective bond orders given in the diagram. Detail description of the natural hybrid orbitals for each bond in resonance form (a) is given in Table 4. Each bond is presented as σ- and/or π-bond. The hybrid orbitals represented at each atom is also listed. The percentage contribution from each hybrid orbital along the bond is also given in this table. The bond order of Ni−N is actually an average value between Ni−N1 and Ni−N2 bonds, i.e., a combination of a dative and a covalent bond character. The π-electron delocal-

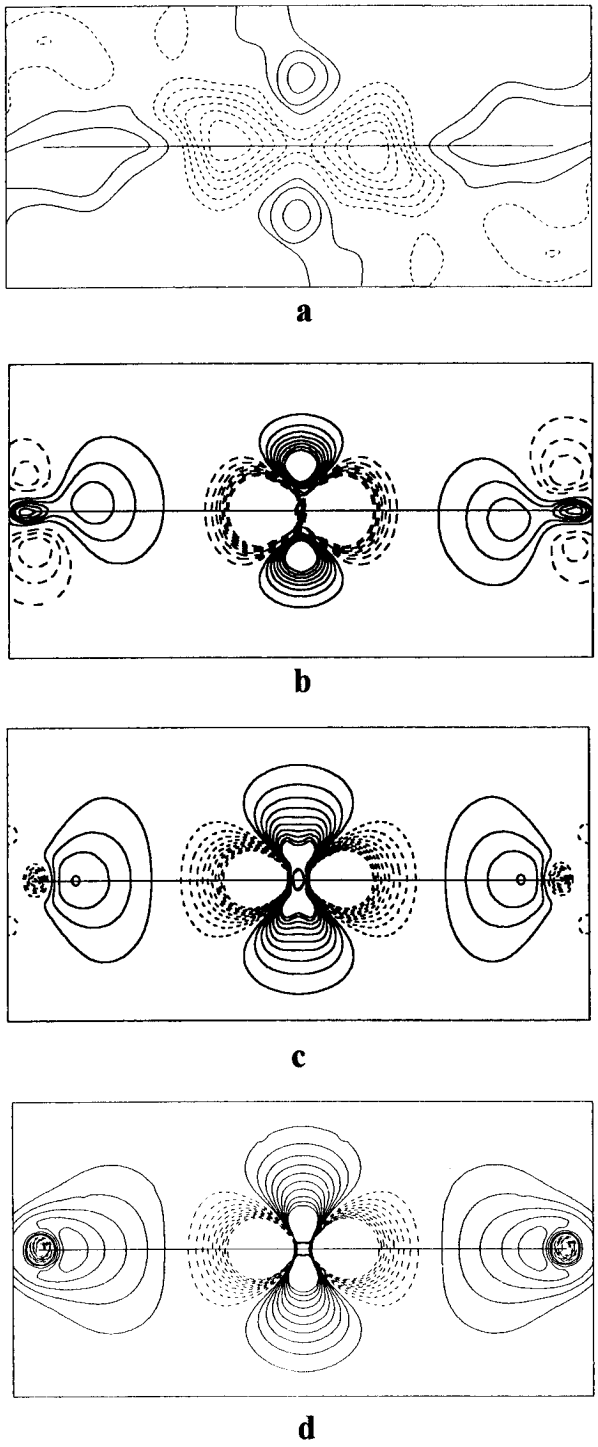

Figure 4. Deformation density maps of the plane perpendicular to Figure 2 and through N1−Ni−N1 atoms; contours as in Figure 3. (a) $\Delta\rho_{x-x}$; (b) $\Delta\rho_{m-a,static}$; (c)$\Delta\rho_{ab\ inito}$; (d) $\Delta\rho_{DFT}$.

ization can also be expressed by the resonance between these three forms (Figure 8).

Atomic Charge and d-Orbital Occupancies. Net atomic charges can be obtained from the least-squares refinement allowing the atomic charge to be redistributed in the molecule according to the multipole model. They can also be obtained from the molecular orbital calculations based on the commonly used Mullikan population analysis (MPA), the natural orbital population analysis (NPA)[29] and the Hirshfeld partition.[28] The results are compared in Table 5. The most negatively charged atoms in the molecule are four imino nitrogen atoms, which are as expected. When we consider the molecule to be

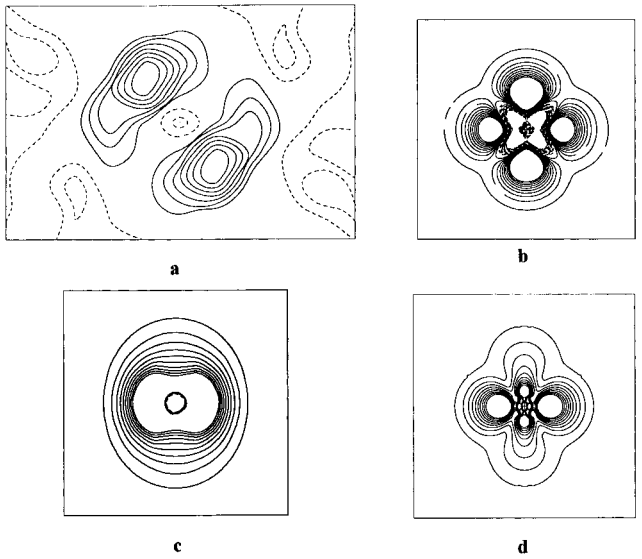

Figure 5. Deformation density maps of the plane perpendicular to Figure 2 and at the bisection of ∠N1−Ni−N2; contours as in Figure 3. (a) $\Delta\rho_{x-x}$; (b) $\Delta\rho_{m-a,static}$; (c)$\Delta\rho_{ab\ inito}$; (d) $\Delta\rho_{DFT}$.

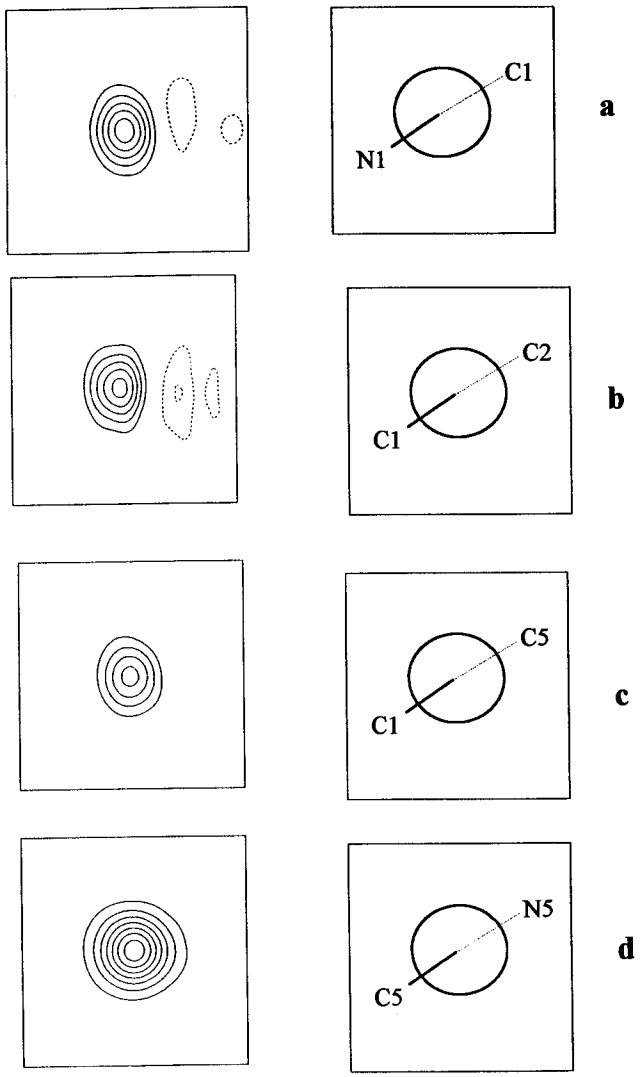

Figure 6. Deformation density maps $\Delta\rho_{m-a}$ of the plane perpendicular to the molecule at the midpoint of (a) C1−N1, (b) C1−C2, (c) C1−C5, and (d) C5−N5 bonds; contours as in Figure 2.

composed by a Ni(II) ion and two s-disn monoanion ligands: the isonitrilo CN is slightly negative, which is neutralized by the attached carbon atoms in the five-membered ring (C1, C2).

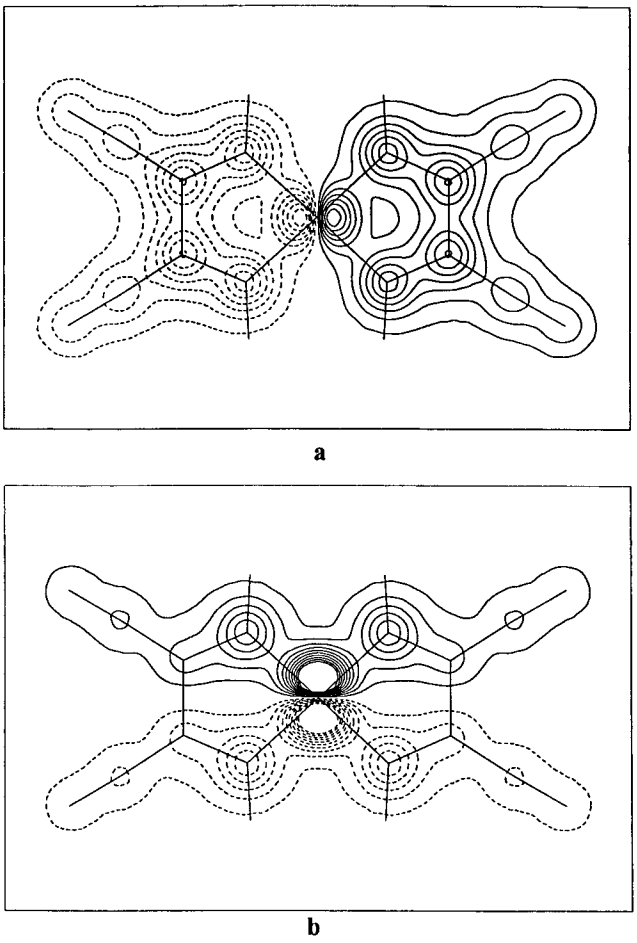

Figure 7. Wave functions of two delocalized π-molecular orbitals (a, b); contours are taken at 0.5 Å above the molecular plane. Solid line positive, dotted line negative.

TABLE 4: Natural Hybrid Orbitals(NHO) and Bond Occupancies(Occ)

bond	NBO type	occu	center	NHO
Ni−N1	σ	1.969	Ni	sd_{xy}(8%)
			N1	sp_xp_y(92%)
Ni	$n1$	1.999	Ni	d_{z^2}(100%)
	$n2$	1.987	Ni	d_{yz}(100%)
	$n3$	1.983	Ni	$d_{x^2-y^2}$(100%)
	$n4$	1.938	Ni	d_{xz}(100%)
N2	n	1.815	N2	sp_xp_y(100%)
N1−H1	σ	1.987	N1	sp_xp_y(72%)
			H1	s(28%)
N1═C1	σ	1.987	N1	sp_xp_y(58%)
			C1	sp_xp_y(42%)
	π	1.932	N1	p_z(68%)
			C1	p_z(32%)
C1−C2	σ	1.966	C1	sp_xp_y(50%)
			C2	sp_y(50%)
C1−C5	σ	1.981	C1	sp_xp_y(50%)
			C5	sp_xp_y(50%)
C5≡N5	σ	1.994	C5	sp_xp_y(43%)
			N5	sp_xp_y(57%)
	$\pi1$	1.987	C5	p_xp_y(47%)
			N5	p_xp_y(53%)
	$\pi2$	1.966	C5	p_z(46%)
			N5	p_z(54%)
N5	n	1.975	N5	sp_xp_y(100%)

According to the experimental result, each s-disn group yields a net charge of −0.24e and, in turn, is compensated for by the positive charge of the Ni atom (+0.50e). It is hard to compare the atomic charges derived from different methods or even from different ways of partition. It is known that there is severe limitation[29] on such quantities derived from MPA.

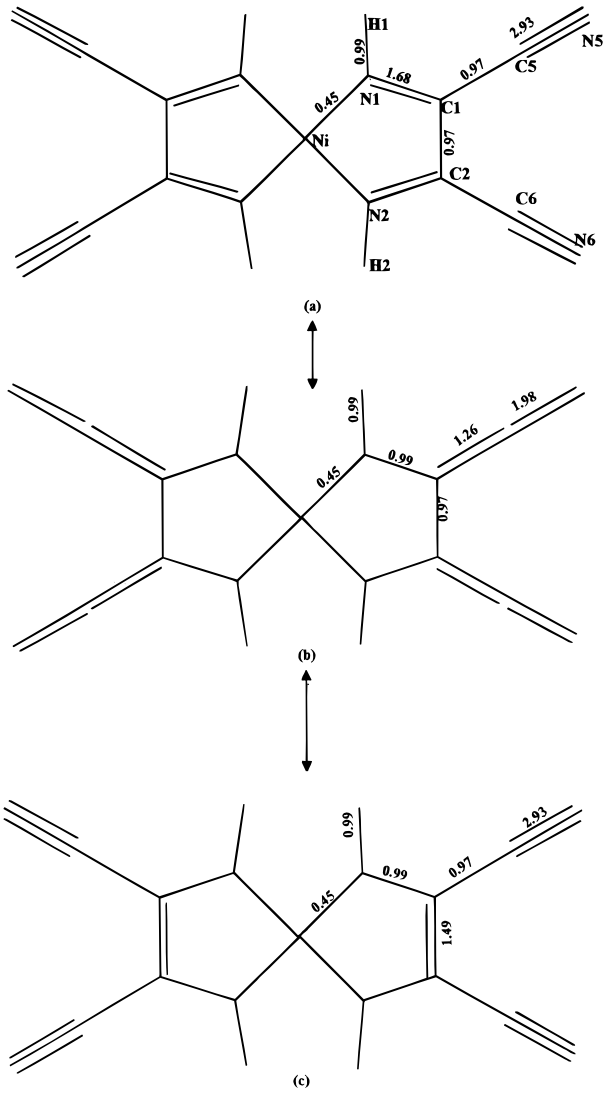

Figure 8. Three resonances forms (a)−(c) from the NBO analysis with respective bond orders.

TABLE 5: Net Atomic Charges

			ab initio		DFT	
	expt	EHMO	MPA	NPA	MPA	Hirshfeld
Ni	0.50(6)	0.17	1.59	1.52	0.16	0.09
N1,N2	−0.36(2)	−0.46	−1.00	−0.92	−0.50	−0.12
N5,N6	−0.30(2)	−0.99	−0.35	−0.29	−0.13	−0.17
C1,C2	0.15(2)	0.42	0.42	0.13	0.16	0.05
C5,C6	0.17(2)	0.77	0.21	0.27	−0.04	0.06
H1,H2	0.22(2)	0.22	0.32	0.44	0.47	0.15

3d orbital populations can also be obtained experimentally by applying multipole refinement and analyzing the multipole coefficients thereafter.[30] The values are listed in Table 6 in comparison to those from MO calculations. The d_{xy} orbital, which is pointed toward four imino nitrogen atoms is least populated, d_{z^2} and $d_{x^2-y^2}$ (nonbonding direction) are mostly populated. Values from the DFT calculation seems to give better (among the MO calculations) agreement with respect to the experimental results. The orbital energies of five d-orbitals should therefore be $E(d_{z^2}) < E(d_{x^2-y^2}) < E(d_{yz}) \leq E(d_{xz}) < E(d_{xy})$. This order conforms to the crystal field theory in D_{2h} symmetry.

A further understanding on the electron density distribution and the bond characterization is currently under investigation via topological studies.

TABLE 6: d-Orbital Occupancies of Ni Atom

					MPA		NPA		MPA	
	expt	%	EHMO	%	ab initio	%	ab initio	%	DFT	%
d_{xy}	0.71	9.21	1.00	11.58	0.33	4.06	0.35	4.27	1.04	12.11
d_{xz}	1.55	20.10	1.81	20.91	1.93	23.74	1.94	23.66	1.73	20.14
d_{yz}	1.76	22.83	1.97	22.68	1.98	24.35	1.99	24.27	1.94	22.58
$d_{x^2-y^2}$	1.82	23.61	1.91	21.98	1.97	24.23	1.98	24.15	1.97	22.93
d_{z^2}	1.87	24.25	1.98	22.85	1.92	23.62	1.94	23.66	1.91	22.24
d_{total}	7.71		8.67		8.13		8.20		8.59	

Conclusion

The combined experimental and molecular orbital calculated electron density study gives clear picture of the bond characters of the molecule. The covalent bonds of triple and partial double C−N bonds are well illustrated. The dative bond character of the ligand imino N atom toward the Ni metal ion is clarified. The complete π-electron delocalization on an s-disn monoanion ligand is incorporated with the Ni d_{xz}, d_{yz} orbitals. The asphericity in density distribution around the Ni atom is well suited for the crystal field theory description of the metal in D_{2h} symmetry. Net atomic charges and d-orbital occupancies derived from the study are quite reasonable. Bond orders are rational from the NBO analysis. The agreement between experiment and theory is encouraging.

Acknowledgment. Financial support of this work from National Science Council of R.O.C. is highly appreciated. Thanks are also due to the National High Performance Supercomputer Center for the use of their computer and softwares.

Supporting Information Available: Anisotropic temperature factors (u_{ij}) of non-H atoms (SI), multipole coefficients (SII), basis functions used in the ab initio calculations (SIII) and in EHMO (SIV), and a complete structure factor list (SV) (5 pages). Ordering information is given on any current masthead page.

References and Notes

(1) Kijma, N.; Tanaka, K.; Morumo, F. *Acta Crystallogr.* **1983**, *A39*, 557.
(2) Yeh, S. K.; Wu, S. Y.; Lee, C. S.; Wang Y. *Acta Crystallogr*. **1993**, *B49*, 806.
(3) Costa, M. M. R.; Paixão, J. A.; De Almeida, M. J. M.; Andrade, L. C. R. *Acta Crystallogr.* **1993**, *B49*, 591.
(4) Byrn, M. P.; Curtis, C. J.; Goldbery, I.; Hsiou,Y.; Khan, S. I.; Swain, P. A.; Tendick, S. K.; Strouse, C. E. *J. Am. Chem. Soc.* **1991**, *113*, 6549.
(5) Kutzler, F. W.; Swepston, P. N.; Berkovitch-Yellin, Z.; Ellis D. E.; Ibers, J. A. *J. Am. Chem. Soc*. **1983**, *105*, 2996.
(6) Maslen, E. N.; Spadaccini, N. *Acta Crystallogr*. **1987**, *B43*, 461.
(7) Miles, M. G.; Hursthouse, M. B.; Robinson, A. G. *J. Inorg. Nucl. Chem*. **1971**, *33*, 2015.
(8) Peng, S. M.; Wang, Y.; Chiang, C. K. *Acta Crystallogr*. **1984**, *C40*, 1541.
(9) (a)Lauher, J. W.; Ibers, J. A. *Inorg. Chem.* **1954**, *14*, 640. (b)Peng, S. M.; Liaw, D. S.; Wang, Yu; Simon, A. *Angew. Chem., Int. Ed. Engl.* **1985**, *24*, 210. (c)Adams, D. M.; Dei, A.; Rheingold, A. L.; Hendrickson, D. N. *J. Am. Chem. Soc.* **1993**, *115*, 8221.
(10) Hansen, N. K.; Coppens, P. *Acta Crystallogr*. **1978**, *A34*, 909.
(11) Stevens, E. D. *J. Am. Chem. Soc*. **1981**, *103*, 5087.
(12) Lecomte, C.; Chadwick, D. L.; Coppens, P.; Stevens, E. D. *Inorg. Chem*. **1983**, *22*, 2982.
(13) Coppens, P.; Li, L. *J. Chem. Phys.* **1984**, *81*, 1983.
(14) Tanaka, K.; Elkaim, E.; Li, L.; Zhu, N. J.; Coppens, P. *J. Chem. Phys.* **1986**, *84*, 6969.
(15) Lecomte, C.; Blessing, R. H., Coppens, P.; Tabard, A. *J. Am. Chem. Soc.* **1986**, *108*, 6942.
(16) Williams, G. A.; Figgis, B. N. *J. Chem. Soc., Dalton Trans*. **1981**, 734.
(17) Figgis, B. N.; Kucharski, E. S.; Reynolds, P. A. *J. Am. Chem. Soc.* **1989**, *111*, 1683.
(18) Li, N.; Su, Z.; Coppens, P.; Landrum, J. *J. Am. Chem. Soc.* **1990**, *112*, 7294.
(19) Albright, T. A.; Hoffmann, R., Thibeault, J. C.; Thorn, D. L., *J. Am. Chem. Soc.* **1979**, *101*, 3801.
(20) (a) Wachters, A. J. H. *J. Chem. Phys*. **1970**, *52*, 1033. (b) Gianolo, L.; Pavani, R.; Clementi, E. G. *Chim. Ital.* **1978**, *108*, 181.
(21) (a) von Barth, U.; Hedin,L. *J. Phys. C* **1972**, *5*, 1629. (b) Versluis, L.; Zeigler, T. *J. Chem. Phys.* **1988**, *88*, 3322.
(22) Vosko, S. J.; Wilk, L.; Nusair, M. *Can. J. Phys*. **1980**, *58*, 1200.
(23) *Gaussian92*, Revision A; Frisch, M. J.; Trucks, G. W.; Head-Gordon, M.; Gill, P. M. W.; Wong, M. W.; Foresman, J. B.; Johnson, B. G.; Schlegel, H. B.; Robb, M. A.; Replogle, E. S.; Gomperts, R.; Andres, J. L.; Raghavachari, K.; Binkley, J. S.; Conzalez, C.; Martin, R. L.; Fox, D. J.; Defrees, D. J.; Baker, J.; Stewart, J. J. P.; Pople, J. A. Gaussian Inc.: Pittsburgh, PA, 1992.
(24) (a) Delley, B. *J. Chem. Phys.* **1990**, *92*, 508. DMol is available commercially from BIOSYM Technologies, San Diego, CA. (b) Delley, B. *Density Functional Methods in Chemistry*; Labanowski, J., Andzelm, J., Eds.; Springer-Verlag: New York, 1991; p 101. (c) Delley, B. *J. Chem. Phys.* **1991**, *94*, 7245.
(25) ICON, Quantum Chemistry Program Exchange, Indiana University, Bloomington, IN.
(26) Restori, R.; Schwarzenbach, D.; Schneider, J. R. *Acta Crystallogr*. **1987**, *B43*, 251.
(27) Foster, J. P.; Weinhold, F. *J. Am. Chem. Soc.* **1980**, *102*, 7211.
(28) Hirshfeld, F. L. *Theor. Chim. Acta* **1977**, *B44*, 129.
(29) Reed, A. E.; Weinstock, R. B.; Weinhold, F. *J. Chem. Phys.* **1985**, *83*, 735.
(30) Holladay, A.; Leung, P. C.; Coppens, P. *Acta Crystallogr.* **1983**, *A39*, 377.
(31) Reed, A. E.; Curtiss, L. A.; Weinhold, F. *Chem. Rev.* **1988**, *88*, 899.
(32) Reed, A. E.; Weinhold, F. *J. Chem. Phys.* **1985**, *83*, 1736.
(33) Löwdin, P. O. *Phys. Rev.* **1955**, *97*, 1474.
(34) Biré, A. S.; Dao, N. Q.; Strich, A.; Thieffry, C.; Bénard, M. *Inorg. Chem*. **1990**, *29*, 4908.
(35) Restori, R.; Schwarzenbach, D.; Schneider, J. R. *Acta. Crystallogr*. **1987**, *B43*, 251.
(36) Gabe, E. J.; Page, Y.; Charland, J.-P.; Lee, F. L.; White, P. S. *J. Appl. Cryst*. **1989**, *22*, 384.

JP951935I